SIFUS: SOAR Integral Field Unit Spectrograph

J.R.D. Lépine[a], A.C. de Oliveira[b], M.V. Figueredo[a], B.V. Castilho[b], C. Gneiding[b], B.Barbuy[a], D.J. Jones[c], A. Kanaan[d], C.M. de Oliveira[a], C. Strauss[a], F. Rodrigues[b], C.R.G. Andrade[b], L.S. Oliveira[b], J.B. de Oliveira[b]

[a] IAG,Universidade de São Paulo, Cidade Universitária, São Paulo, Brazil
[b]Lab. Nacional de Astrofísica, MCT, Itajubá, MG, Brazil
[c]Prime Optics, 17 Crescent Road, EUMUNDI Q 4562 Australia
[d]Univ. Federal de Santa Catarina, Brazil

ABSTRACT

We present the project of an optical spectrograph equipped with a 1300-element Integral Field Unit (IFU), that will be one of the main instruments of the SOAR (4m) telescope. The instrument consists of two separate parts, the fore-optics and the bench spectrograph, that are connected by a 11 m long fiber bundle. The fore optics system is installed at one of the Nasmyth focii of the telescope, and produces an image of the observed object on a 26x50 array of square microlenses, each 1 mm x 1 mm lens feeding one fiber. The fibers have 50 micron cores, and are aligned at the entrance of bench spectrograph to form a slit that feeds a 100 mm beam collimator. A set of Volume Phase-Holographic (VPH) transmission gratings can be interchanged by remote control, providing a choice of resolution and wavelength coverage. The spectrograph is tunable over the wavelength range 350 to 1000 nm, with resolution R from about 5000 to 20000. This spectrograph is ideally suited for high spatial resolution studies, with a sampled area of the sky 8" x 15", with 0.30" per micro lens, in the mode to be used with the tip-tilt correction of SOAR. The project has been approved at the Project Design Review and the spectrograph is presently being constructed.

Keywords: Spectrograph, Integral Field Unit, Volume Phase Holographic

1. INTRODUCTION

The purpose of the spectrograph is to best exploit SOAR's excellent angular resolution (about 0.15 arcseconds, with tip-tilt correction) in cases where complex extended objects or objects in crowded fields are studied. The unit permits simultaneous spectra to be taken of all parts of moderately extended objects like HII regions or distant galaxies. Strong motivations for high spatial resolution are the study of velocity fields and of ionization structure in HII regions, AGNs, and planetary nebulae.

An IFU spectrograph is competitive at this spatial resolution, not only for extended objects but also for stellar spectroscopy. In a slit spectrograph, the slit width must be kept to a minimum to obtain high resolution, but this has the disadvantage of vignetting much of the seeing disk in non-optimal seeing conditions. This limitation does not exist in a IFU spectrograph, since all the light of a star is used. The IFU spectrograph will be especially useful in crowded fields like globular clusters or the Magellanic bar, allowing simultaneous observations of many stars. The spectral resolution (R $=\delta\lambda/\lambda$) is sufficient to study the metalicity of stars (at R > 6000), or abundance ratios like [Hα/Fe] (at R > 15000).

There are already several IFU spectrographs in operation, eg. the TIGER at the CFHT (Bacon et al., 1995), OASIS by the same group, HYDRA at the WIYN telescope (Barden and Armandroff, 1995), WYFOS at the WHT, etc), VIMOs at the VLT (Le Fevre et al. 2000), and GMOS at GEMINI (Davies et al. 1997). The main characteristics that turn the present instrument a competitive one are: 1) the wide wavelength coverage, from 350 to 1000 nm, 2) the use of small diameter fibers, which allows efficient packing at the slit, and the use of optics with relatively modest beam diameter 3) interchangeable fore-optics magnification 4) the use of

J.R.D. Lépine: E-mail: jacques@astro.iag.usp.br

interchangeable VPH transmission gratings, that offer a range of resolutions ($\delta\lambda/\lambda$)from about 5,000 to 30,000, and 5)the relatively large efficiency, obtained by the choice of materials, reduced number of lenses, and Sol-Gel coating.

The concept and construction of this spectrograph largely benefited from the experience of the Australian spectrograph SPIRAL and it Brazilian version Eucalyptus, considered as a prototype for the present instrument. The Eucalyptus spectrograph is also described in these proceedings (A.C. de Oliveira et al.).

2. OPTICAL DESIGN

2.1. The fore-optics

The micro lens-fiber IFU is coupled to the telescope via simple fore-optics. The function of the fore-optics is to magnify the focal plane of the telescope to the scale that is required by the micro lens array. The fore-optics consists of a magnification lens and a field lens. The field lens is used to provide telecentric correction to the magnified beam; that is, the light must feed the lenses parallel to their axes.

Two interchangeable sets of lenses with different magnifications will be available, so that the system can be adapted for relatively bad seeing conditions (still good for stellar spectroscopy) and/or observations covering a larger field, and for observations in the blue region. The first goal is to match 0.15" of the sky, or 49 μm in the focal plane, to the 1 mm lenses; this corresponds to a magnification of about 20. In the red part of the spectrum, the PSF with tip-tilt correction is expected to be about 0.30", so that this choice corresponds to ideal spatial sampling by two microlenses.The second fore-optics system has a magnification a factor 2 smaller than the first one, resulting in 0.30" per lens. To make provision for a 0.08"/pixel scale to be used with Adaptative Optics, we leave room for a third switchable magnification, on a sliding system with room for three sets of fore-optics lenses. It might be interesting to have an option for 0.60" per pixel, but this cannot be obtained without some loss of light (the image of the pupil at the input of the fibers would be larger than the core diameter, unless we use a different core diameter). For the moment, we leave as future options the possibilities of 0.08" or 0.60" per pixel.

2.2. The IFU

The IFU is composed of the crossed cylindrical lenses from the German company LIMO (Lissotschenko Mikrooptik); see Figure 1. The cylindrical lenses are manufactured with aspheric surface profiles producing diffraction limited performances, and the array is made achromatic with the use of a high dispersion glass substrate, ensuring high throughput at all wavelengths.

The coupling of fibers to the lenslet arrays will use the technique which was used for the Eucalyptus spectrograph (A.C de Oliveira et al., this conference). The fibers extremities are introduced and cemented in steel jackets (steel tubes used for hypodermic needles). The jackets are introduced in an array of holes in a metal block, and are all polished simultaneously. The fibers are fixed on the glass substrate with UV-cured cement.

2.2.1. The sky IFU

For observations of extended objects, sky subtraction is a major concern, since very often, regions of the sky not contaminated by the object are only found at distances larger than the size of the IFU. One mode of observation (see section 3) uses for sky subtraction a separate IFU with a small number of pixels (5 x 5), positioned in the sky at about two arc minutes from the object. The "sky" IFU will be built with the same technology of the main one, since we desire similar transmission for the sky and the object. In our case, due to the relatively small diameter of the pick-off mirror, the sky IFU cannot go far from the main IFU. To observe the sky at 2' from the main IFU, we must install another fore-optics first lens at about 50 mm from the interchangeable ones, and therefore, to have a completely independent fore-optics system. To avoid too many controls or duplicate optical systems, our choice is to have a fixed position of the sky IFU, and a single magnification (factor 10). A rotation of the plane of the sky, performed by the ISB, will allow in most cases to find a convenient position in the sky for the sky IFU. The question of different magnifications between object and sky, when the factor 20 magnification is used at the main IFU, can be corrected during data reduction, using a correction factor derived from the flat field.

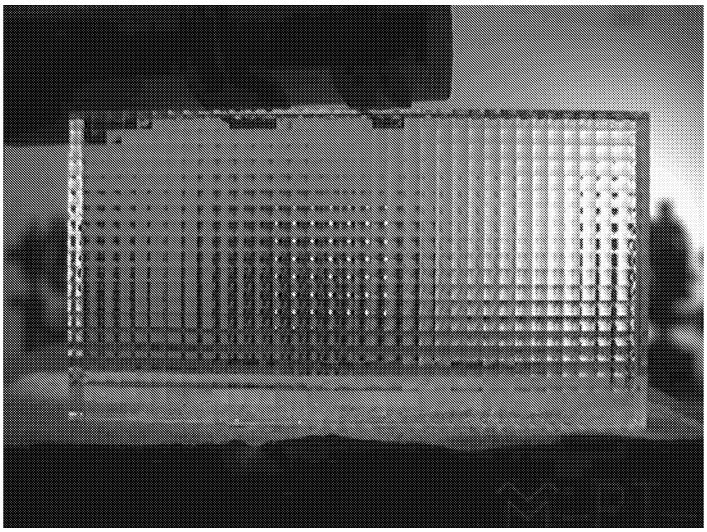

Figure 1. An array of square 1 mm x 1 mm microlenses from LIMO.

2.3. The fibers

We use Polymicro "blue" fibers; their transmission curve is shown by the dashed curve in Figure 2. The reason for this choice is that they are much better in the blue than low-OH fibers, which would turn impossible observations at 350 nm. We need at least 5 μm cladding thickness, to avoid light loss at the longest wavelength (1 μm). The "blue" fibers present a deep absorption at about 950 nm. Since it coincides with an atmospheric absorption, it is not a region of interest for observations. We intend, after the start of the use of the spectrograph, to construct a second fiber bundle optimized for the red /near-infrared region. We use 50 μm fibers, with 5 μm thick cladding. This preserves the minimum cladding thickness/wavelength ratio of 5:1 at 1 μm, with a usual 10:1 core/cladding ratio. The center-to-center separation will be 75 μm, and the total height of the 1300 fibers column will be 98 mm. This determines the diameter of the beam about 100 mm, and the focal length of the collimator about 500 mm.

2.4. The slit and the collimator

After many efforts to optimize a dioptric collimator, a new catadioptric collimator has been developed to circumvent the chromatic problems. This collimator delivers near diffraction-limited imagery over almost the entire slit field from a wavelength of 290 nm to 2500 nm. It is used in an off-axis, unobscured, mode that is identical, in principle, to the 2dF spectrograph collimators on the Anglo Australian Telescope (Lewis et al. , 2002). The slit surface is convex to the collimator with a radius of curvature of about 500 mm. There is a fused Silica cover plate that also contributes to aberration control.

Although the slit surface is coaxial with the rest of the system, the excentric entrance pupil means that the fiber ensemble must be inclined by nearly 6 degrees with respect to the plane containing the slit itself and the system optical axis. This is identical in principle, again, with 2dF.

The reversed collimator is an off-axis section of a symmetric system of focal ratio 2; it is a catadioptric system having characteristics of both Maksukov and Houghton systems. It contains 3 weak elements of fused silica. The two negative meniscus elements are each similar to a Maksukov corrector whilst the positive element is similar to part of a Houghton corrector doublet. The collimator has, in fact, been designed as an imager, or reversed collimator. The 3 elements are necessary for full control of the field aberrations over the full length of the slit. There is a cover on the slit surface which also contributes to aberration control.

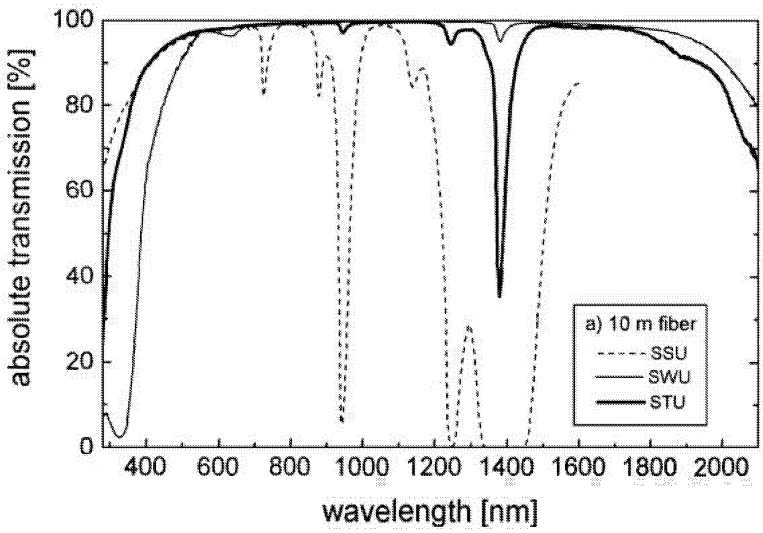

Figure 2. Transmission curves of high-OH or "blue" fibers (SSU), low-OH or "red" fibers (SWU), and fluosil fibers. Our choice for the first IFU-fibers system is the SSU fibers.

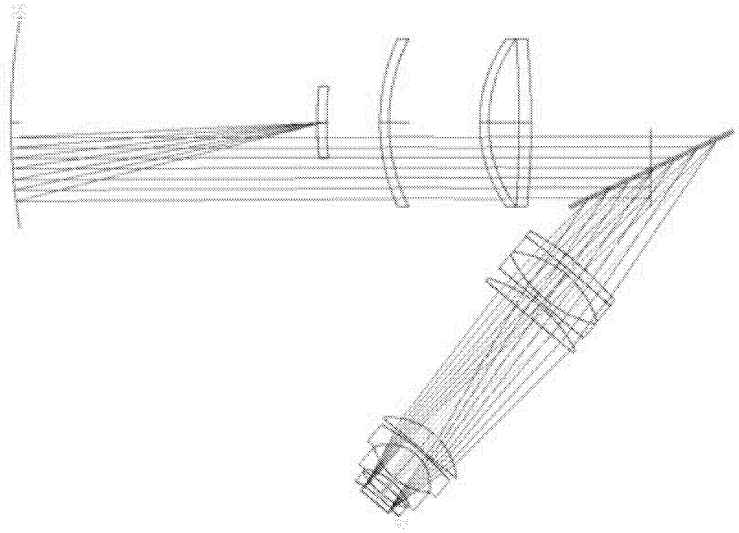

Figure 3. Collimator, grating and camera, in a situation with large diffraction angle. In the collimator, only the section of the lenses with the diameter of the beam will be constructed.

2.5. The camera

The SIFUS camera is an all-refracting (dioptric) design based on a field-flattened Petzval configuration. The positive power is distributed among 4 components so as to ease the control of aberrations. Several glasses are used to control secondary (and higher order) chromatic aberration (color). This is the limiting aberration in systems of this type, especially when extended into the UV. The selection of useful glasses is extremely limited and there are increasingly significant penalties in UV transmission as the selection is broadened.

The "core" system can be thought of as essentially 2 singlets of Calcium Fluoride (CaF2) enclosed by 2 doublets of CaF2/Schott BaK2. An extra "flint" element of OHARA BAL51Y is added to one of these doublets to enhance the control of spherical aberration and longitudinal color.

The other doublet also has a weak "flint" addition of Schott LLF2. This is added to better control secondary color, both lateral and longitudinal. The negative field flattener is also a "flint" (SILICA) which further improves the correction of lateral color.

The collimator, grating and camera arrangement are shown in Figure 3.

3. THE VPH GRATINGS

The VPH gratings are not too expensive, and we could think in terms of a reasonable number of gratings that can be simultaneously installed in the bench spectrograph and remotely interchanged. From our study of efficiency and resolution as a function of wavelength, we consider that 6 gratings are required to reach the specifications of the spectrograph. We next present the set of 6 VPH gratings. The studies were made with the software G-Solver, which is based on Rigorous Coupled Wave Analysis. The angle of the grating and of the camera must be tuned independently to get maximum efficiency at a given wavelength. We always use first order, and do not consider using the gratings at efficiency lower than 50%.

We considered that the grating will always operates near the Bragg, regime, in which the deflection angle is equal to the angle of incidence as shown in the figure presenting the optics. The resolution that we present corresponds to 2 pixels, since the image of the output of a fiber matches 2 pixels of the CCD.

A resolution R = 30 000 is reached at an incidence angle of 53.7°. This does not depends on the characteristics of the grating. The grating must be sufficiently wide to intercept the beam without vignetting; for a 100 mm beam this implies a 100 x 169 mm grating.

The proposed set of gratings enables us to reach resolution higher than 20,000 over a large fraction of the 350-1000 nm range, and at the same time to provides a wide range of resolutions. The lowest resolution allows us to cover the whole wavelength range in two steps, and the highest resolution reaches about 50,000 at Hα, which is convenient for velocity measurements. The parameters that were adjusted to obtain best efficiency at each wavelength coverage are the groove density, the amplitude of modulation δn of the index of refraction, and the thickness of the gel layer (see Table 1).

Table 1. Characteristics of the gratings

Frequency (gr/mm))	δn (for n=1.5)	d(μm)
500	0.040	9.1
1300	0.075	4.0
1800	0.075	4.0
2200	0.070	5.0
2600	0.05	5.5
3600	0.044	4.0

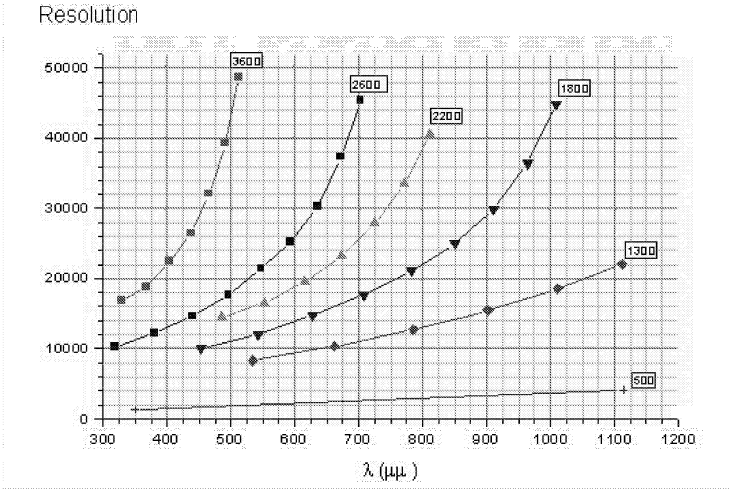

Figure 4. The resolution ($R = \delta\lambda/\lambda$) is shown as a function of wavelength for 6 different VPH transmission gratings (the number of grooves/mm is indicated for each one).

4. EFFICIENCY

The overall efficiency at a given wavelength is obtained by multiplying the efficiency of each component. Since the efficiency strongly decreases at wavelengths shorter than 350 nm (see eg. the efficiency of the fibers in Figure 2), we present in Table 2 the contributions to light loss at this limit wavelength. Our calculations do not include atmospheric absorption, of the order of 0.7 at 350 nm. One can see that one of the few factor we can expect to improve is the focal ratio degradation in the fibers (part of the light of the fiber output does not enter in the collimator because of too large divergence of the beam). This focal degradation was measured for the fibers used in the prototype; we expect to obtain a better figure in the present spectrograph by avoiding stress in the fibers.

Table 2. Contributions to the overall transmission efficiency

Telescope	80 %
Fore-optics	90 %
Fiber transmission	85 %
Loss due to F.R. degrad	70 %
Spectrograph transmission	70 %
Grating efficiency	70 %
CCD	70 %
TOTAL	15 %

5. THE MECHANICAL DESIGN

The mechanical project comprises two well separated parts, the fore-optics box and the bench spectrograph.

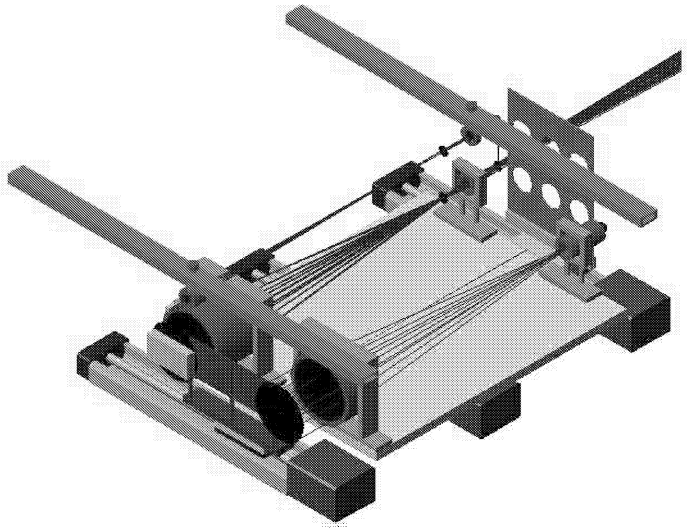

Figure 5. The fore-optics box contains a sliding plate to remotely interchange sets of lenses with different magnifications. The plate for filter interchange can be seen. The micro lens array is represented as a block in front of the optics in use.

5.1. The fore-optics box

The fore-optics box is mounted on a side of the Instrument Selector Box of the telescope, using a flange with bolts. The fore-optics box contains the following main components:
1) a movable plate, operated by remote control, supporting the two interchangeable sets of fore-optics lenses that provides the different magnifications (see section 2 for a discussion of the optics). There is room for an additional fore-optics system, that could be useful if the system is to be used with adaptative optics in future.
2) a third fore-optics system for the sky IFU, which is not movable. It is suspended "above" the interchangeable fore-optics, in such a way that it does not limit the access to adjust or align the main fore-optics.
3) a sliding plate that allows 3 different Shot filters and a blank space to be interchanged by remote control. Note that the focus of the telescope is 150 mm outside the external surface of the ISB. The filter plate is placed in this space, before the magnification lenses.
4) a mask, very close to the micro lens array, that can slide and presents different options, like full illumination of the array, illumination of only half of the array for shuffle- and- node observations, or a set of holes that allows only a number of lenses of the array to be illuminated, in order to study the profile of the image of individual fibers on the CCD. The mask is remotely controlled.
5) an adjustable system to hold the micro lens arrays, able to provide alignment of the arrays with the fore-optics. This is a critical adjustment, but it does not require remote control.

Although a same field lens is designed for the two fore-optics sets with different magnifications, it is not situated at the same distance of the micro lens array in the two cases. We prefer to duplicate the field lens, so that a single lateral displacement of the supporting plate changes the whole set, magnification lenses plus field lenses.

In summary, 3 systems mounted on sliding rails are remotely controlled, for the interchange of fore-optics, of filters and of masks. The interior of the fore-optics box is illustrated in Figure 5. Note the sky fore-optics, hanging above the main fore-optics in use.

The micro lens holder, fiber bundle, stress-release box, will be very similar to those of the prototype (the Eucalyptus spectrograph, also presented at this conference).

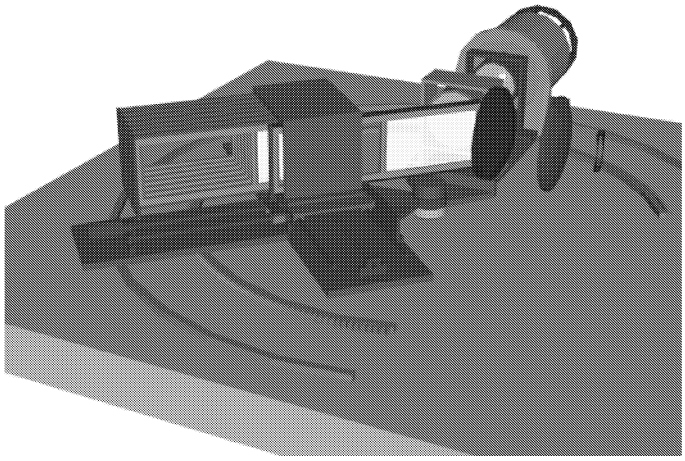

Figure 6. The grating exchanger mounted on a rotating support on the bench

5.2. The bench spectrograph

The bench spectrograph will be installed on the platform of the telescope, which is part of the azimuth mount. The spectrograph is mounted on a 2.4m x 2.4m table of aluminium honeycomb structure with 150 mm thickness, supported by 4 pneumatic short legs for vibration isolation. The whole spectrograph will be covered with a removable aluminium cover that will isolate it from external light. The internal part of the cover will be covered by thermal insulating material, to avoid fast changes in temperature.

The fiber slit is mounted on a system that allows fine adjustment of the position and angle of the slit. The collimator mechanical parts are usual lens supports, directly fixed on the bench, with capability for optical alignment.

Independent rotation of the transmission gratings and of the camera, is provided by two independent support plates that share a same central axis and a same circular rail. Usually, the camera is placed at an angle about twice the angle of the grating, with respect to the beam coming from the collimator, in order to be close to the Bragg condition. The two independent plates can rotate around the central axis that passes through the center of the grating which is being used. On their external parts, the plates are supported by a rolling ball systems (two for each plate) that run on a circular rail. The next figures illustrate this geometry.

The rotation of the grating exchanger and of the camera is provided by two similar systems, with a motor that rotates an endless screw mounted under each plate, running along a common toothed ring fixed on the bench. The maximum angle of the camera will be about 67 o. Absolute encoders mounted on the rotation axis will provide reading of the angle of the camera and of the grating.

An important component is the grating exchanger, which looks like the carriage of a slide projector. It is able to offer a choice of 8 gratings (possibly at the beginning of the operations only a smaller number will be available). Two sliding systems, based on THK stages, are needed to change the gratings: the first one moves the grating carriage in order to place the selected grating at the position of the second one, and the second one moves in and out the selected grating.

6. OBSERVATIONS AND DATA REDUCTION

6.1. Observation modes

Two main modes of observations will be available:
1)Normal integration, with sky subtraction using the sky IFU, or with separate integration on the sky.

2)Nod-and-shuffle observations.

The first mode is convenient to take advantage of the full spatial coverage of the IFU, which is important for extended objects. It will be usually possible to place the sky IFU, situated at 5' from the main IFU, in a region free of object emission. The variability of the sky emission is taken into account, since the sky is observed simultaneously with the object. The idea, then, is to compute the median of the 25 sky spectra and subtract it from each 1300 object spectra. Differences in transmission from individual fibers can be compensated, using relative transmission factors obtained from flat field measurements. The accuracy of the sky subtraction is expected to be of the close to 1, based on the experience of other groups. Our experience with the prototype is that the relative transmission of the fibers is very stable, even with strong curving of the fiber bundle.

When a mosaic of many exposures of an extended object is performed, it may be interesting to take one or two exposures of the sky with the main IFU. In this way direct subtraction can be performed, that takes into account in a simple way of differences in fiber transmission and wavelength shifts.

When very accurate sky subtraction is required, like for instance for faint objects, the nod-and-shuffle mode is probably better. In this mode, a mask is used in front of half of the lens array, and only a square region of 26x25 array elements will be used. Therefore on the CCD, groups of 25x3 lines corresponding to the observed region are alternated with groups of the same number of lines without signal. The telescope is switched between the object and a sky position, every 60 seconds, and at the same time, the charges are shuffled 75 lines on the CCD. The sky integration starts over the charges that where previously in the masked regions. After 60 seconds the charges are moved back to their previous positions and the telescope returns to the object. After 30 minutes of observations, the CCD contains 15 minutes of object integration and 15 minutes of sky observation that can be directly subtracted. The advantage is that for each spectrum, the sky is obtained with the same fiber and same pixels. This mode is useful when the sky is stable (no clouds).

6.2. Data Reduction

We intend to provide the means for doing quick look at the telescope and the data reduction software to reduce the data during the observation run or in the next days. The reduction data software for SIFUS is in development and will be detailed in a forthcoming paper. The software will be shared with Eucalyptus (see de Oliveira et al., in this conference for a description of the software and of Eucalyptus), for which a beta release should be operational in two months for the first scientific programs. The software will be constructed under IFRAF, because it is a free and supported platform, and most of SIFUS and Eucalyptus users are familiar with it. The only step that is specific to SIFUS and Eucalyptus reduction is the extraction of the fiber spectra from the initial CCD image. It is expected that everything else could be done using standard IRAF packages with minor modifications. As for looking at the final 3D data, there are also existing packages that can do this. We intend to develop a task similar to 'ldisplay' in the 'gmisc' package as a quick look tool.

ACKNOWLEDGMENTS

The project is in large part funded by the São Paulo State agency FAPESP. It benefited from helpful advice from Tom Ingerson (ex-member of CTIO), David Lee (AAT), Keith Taylor (ex-member of AAT), Damien Jones (Prime Optics, responsible for the optical design), Chris Clemens (UNC, expertise on VPH gratings), Steve Heathcote (Director of SOAR Observatory), Fernando Santoro (mechanical design, presently at CTIO).

REFERENCES

1. Bacon, R., et al., 1995, AAS 113, 347

2. Barden, S.C.; Armandroff, T., 1995, Proc. SPIE Vol. 2476, p. 56-67, Fiber Optics in Astronomical Applications, Samuel C. Barden; Ed.

3. Davies, R. L.,et al., 1997, Proc. SPIE Vol. 2871, p. 1099-1106, Optical Telescopes of Today and Tomorrow, Arne L. Ardeberg; Ed.

4. Le Fevre, O., 2000, Proc. SPIE Vol. 4008, p. 546-557, Optical and IR Telescope Instrumentation and Detectors, Masanori Iye; Alan F. Moorwood; Eds.

5. Lewis, I. J, et al., 2002, MNRAS 333, 279